Biosensors and Bioelectronics 142 (2019) 111482

Contents lists available at ScienceDirect

Biosensors and Bioelectronics

journal homepage: www.elsevier.com/locate/bios

An affinity peptide-incorporated electrochemical biosensor for the detection of neutrophil gelatinase-associated lipocalin

Chae Hwan Cho[a,1], Ji Hong Kim[a,1], Dae-Kyu Song[b], Tae Jung Park[c,**], Jong Pil Park[a,*]

[a] Department of Pharmaceutical Engineering, Daegu Haany University, Gyeongsan, 38610, Republic of Korea
[b] Department of Physiology, Keimyung University School of Medicine, Daegu, 12602, Republic of Korea
[c] Department of Chemistry, Institute of Interdisciplinary Convergence Research, Research Institute of Halal Industrialization Technology, Chung-Ang University, 84 Heukseok-ro, Dongjak-gu, Seoul, 06974, Republic of Korea

ARTICLE INFO

Keywords:
Neutrophil gelatinase-associated lipocalin
Peptide receptor
Sensitivity
Electrochemical sensor

ABSTRACT

In this study, we demonstrate a novel affinity peptide-incorporated electrochemical biosensor for the detection of acute kidney injury and the diabetic biomarker neutrophil gelatinase-associated lipocalin (NGAL). Biopanning of the M13 phage display library over immobilized NGAL led to the rapid identification of unique affinity peptide with an amino acid sequence of DRWVARDPASIF, and the peptide-displayed phage particles were found to be specific affinities for NGAL. To address the development of peptide-based electrochemical sensor, a series of synthetic peptides away from phage particles was rationally designed, chemically synthesized, and immobilized to a gold sensor layer. Among five synthetic peptide derivatives tested, NGAL BP1 was selected as most promising recognition receptor, and its binding affinity was monitored by SWV and EIS. Using EIS, the limit of detection (LOD) was 1.74 ng/mL, while SWV had a LOD of 3.93 ng/mL. The detection performance of the peptide-incorporated sensor was comparable to commercially available ELISA NGAL detection kits. In addition, the validation of the peptide sensor was also confirmed with plasma from patients, and it was observed that the sensitivity of the peptide sensor showed a statistically significant difference. Our results show that the phage and peptide sensor system could detect NGAL with high sensitivity and selectivity, and this suggests its potential use as a biosensing platform for monitoring NGAL in a miniaturized electrochemical biosensor.

1. Introduction

Acute kidney injury (AKI), a complex, heterogeneous, and asymptotic disease, is a leading cause of death in many countries (Bonventre, 2007; Coca et al., 2008; Han et al., 2008; Pal et al., 2016; Soni et al., 2009). Therefore, there is an increasing demand for developing precise methods for its early diagnosis. Several clinical serum and urine biomarkers have been identified and systemically characterized for the early diagnosis of AKI (Belcher et al., 2014; Hassanzadeh and Ghaemy, 2017; Mousavi et al., 2015; Parmar et al., 2016), and the measurement of serum creatinine level is the gold-standard method for diagnosing it (Pal et al., 2016; Parmar et al., 2016). However, the serum creatinine level can depend on several factors, including body weight, age, gender, drug treatment, and chronic kidney disease development (Mousavi et al., 2015). Therefore, AKI diagnosis based on it should be clinically validated and practiced to achieve the best outcomes.

Over the past few years, neutrophil gelatinase-associated lipocalin (NGAL) has emerged as a promising biomarker for AKI diagnosis possibly because of its high selectivity and reliability (Barrera-Chimal and Bobadilla, 2012; Coca et al., 2008; Endre and Pickering, 2014; Li et al., 2015). Urinary albumin excretion is a major product of both glomerular and tubular pathology, suggesting that a more specific biomarker for tubular injury is needed. It is elevated in type 1 diabetes and increases significantly with increasing albuminuria (Bjornstad et al., 2018; Sheanon et al., 2018). Recent studies have demonstrated the association between early tubular lesions in nonalbuminuric patients with type 1 diabetes and NGAL (Bjornstad et al., 2018; McCullough et al., 2013; So Young et al., 2018; Soni et al., 2009; Waikar and Bonventre, 2007). From these facts, diagnosis based on NGAL level can assist in the early identification of high-risk patients with diabetes and AKI and thereby ensure the early detection of AKI and/or prevention of diabetic nephropathy.

* Corresponding author.
** Corresponding author.
E-mail addresses: tjpark@cau.ac.kr (T.J. Park), jppark@dhu.ac.kr (J.P. Park).
[1] These authors were equally contributed to this work.

https://doi.org/10.1016/j.bios.2019.111482
Received 11 May 2019; Received in revised form 24 June 2019; Accepted 26 June 2019
Available online 28 June 2019
0956-5663/

Several NGAL immunoassays for AKI diagnosis are available commercially. Alere Triage NGAL assay has a detection limit of ≤10 ng/mL for NGAL concentrations ranging from 20 to 200 ng/mL in whole blood or urine sample (Ribitsch et al., 2017), which provides the best performance with high sensitivity and specificity within a short time (15 min). However, most available assays for detecting NGAL levels primarily rely on antibodies as biorecognition elements and involve multistep sample preparation and (in some cases) appropriate labeling processes (Lee et al., 2018). The production of antibodies is relatively expensive, and they easily lose their binding properties under unfavorable conditions (Hwang et al., 2015; Yang et al., 2018; Yoon et al., 2017) and additionally show some cross-reactivity. To address these limitations, various effective affinity reagents, including aptamers (Crivianu-Gaita and Thompson, 2016), peptide nucleic acids (Teengam et al., 2017), peptides (Hwang et al., 2015), and other assay materials (Park et al., 2018; Yukird et al., 2017), have been developed. Among these, peptides are an attractive option because their synthesis is cost-effective and they are more stable than antibodies, suggesting that they can be used in biosensor applications (Heo et al., 2019; Hwang et al., 2017; Park et al., 2015). Phage display is a powerful technique for identifying unique short consensus peptide motifs that bind to targets, including inorganic materials or disease biomarkers (Hwang et al., 2017; Ki et al., 2010; Yoon et al., 2017). Peptides isolated using the M13 phage display library or peptide-displayed phages have been used as alternatives to antibodies for developing bio-imaging probes, which are novel scaffolding materials for various applications (Sidhu et al., 2007; Wu et al., 2011).

Electrochemical detection is widely used in the development of label-free and portable biosensors in point-of-care testing (Hwang et al., 2017). This is a promising and cost-effective method for developing biosensors due to its quick response time and low maintenance. Cyclic voltammetry (CV) is one of the most interesting methods because it is a label-free and fast response for measurement (Hwang et al., 2017; Park et al., 2018). Electrochemical impedance spectroscopy (EIS) is also widely used in biosensors because of its rapid response time and reliability, and because it allows label-free detection (Wu et al., 2011). Thus, both CV and EIS are feasible and straightforward detection tools for monitoring various analytes (Wu et al., 2011). Another electrochemical detection methods including ion-sensitive field-effect transistor (IS-FET) are also widely used for biosensor application (Choi et al., 2019; Tai et al., 2019).

In this study, we used a polyvalent phage display technique as screening tool to identify novel affinity peptides that could bind to NGAL and electrochemical detection method as monitoring tool for the development of peptide-incorporated biosensor. After five rounds of biopanning, high-affinity peptides were screened, and the performance of an electrochemical phage sensor containing an NGAL-specific peptide was determined by performing enzyme-linked immunosorbent assay (ELISA), CV, SWV, and EIS. We utilized a polyvalent phage display which is 5 copies of the peptide per phage and the interaction of peptides with NGAL protein may be different when the peptides away from phages are immobilized on gold surface with different density. Therefore, synthetic peptides were rationally designed, chemically synthesized, and covalently immobilized to a gold sensor layer for the development of peptide-incorporated electrochemical sensor (Scheme 1). To the best of our knowledge, this is the first study to identify and characterize newly identified affinity peptides for detecting NGAL in a miniaturized electrochemical phage and peptide biosensor system.

2. Materials and methods

2.1. Chemicals

Recombinant NGAL was purchased from Randox (Crumlin, UK). Tween 20, and the diammonium salt of 2,2′-azino-bis(3-ethylbenzothiazoline-6-sulfonic acid) were purchased from Sigma-Aldrich (St. Louis, MO, USA). Horseradish peroxidase (HRP)-conjugated anti-M13 monoclonal antibody was purchased from GE Healthcare (Piscataway, NJ, USA). A Coomassie protein assay kit and streptavidin-coated microwell plates were obtained from Pierce Biotechnology (Rockford, IL, USA). Unless otherwise stated, all chemicals were of reagent grade. Gold (III) chloride trihydrate and sodium citrate dehydrate were purchased from Sigma-Aldrich. An ELISA NGAL detection kit was purchased from R&D Systems (catalog number: DLCN20, Minneapolis, MN). A series of synthetic peptides (NGAL binding peptide 1–5 (BP1–BP5) was chemically synthesized by Peptron (Daejeon, Korea) and modified with C-terminal cysteine and a linker (-GGGGS-) for molecular flexibility. The protocol for obtaining and utilizing human serum samples from patients was approved by the ethics review committee of the Institutional Review Board, College of Medicine, Keimyung University.

2.2. Escherichia coli strains and peptide library

E. coli ER2738 strains used as hosts for M13 phage infection and the M13 random peptide library (Ph.D.-12) were obtained from New England Biolabs (Ipswich, MA, USA).

2.3. General M13 phage preparation and DNA sequencing analysis

Phage purification, concentration, and DNA isolation were carried out according to the manufacturer's instructions. Single-stranded DNA samples from positive phages were sequenced by Genotech (Daejeon, Korea) using −96 pIII sequencing primer 5'-CCCTCA TAGTTAGCGTA ACG-3'. BLAST searches were performed using the SWISSPROT database to determine sequence similarity with previously identified peptides or proteins. The Clustal Omega program (http://www.ebi.ac.uk/Tools/msa/clustalo/) and ExPASy tools (web.expasy.org/translate) were used to analyze the sequences.

2.4. Evolutionary screening of affinity peptides (biopanning)

Biotinylated NGAL was dissolved in 50 mM Tris-HCl (pH 7.0) and transferred to the wells of 96-microwell plates. After overnight incubation at 4 °C with mild shaking, the pre-immobilized wells were filled with blocking buffer (0.1 M $NaHCO_3$ (pH 8.6), 5 mg/mL of bovine serum albumin (BSA), and 0.02% NaN_3), and incubated at 4 °C for 1 h. After removing the unbound and residual blocking solution, wells were washed six times with TBST buffer (50 mM Tris-HCl (pH 7.5), 150 mM NaCl, and 0.1% Tween 20). The Ph.D.-12 random peptide library (1.5×10^{13} pfu) was added to the pre-immobilized wells, and the plate was shaken gently for 1 h at room temperature. To remove unbound phages, the plate was washed 10 times with TBST. Three rounds of biopanning were performed against recombinant NGAL proteins. After washing, the bound phages were eluted using 100 μL of 0.2 M glycine-HCl (pH 2.2), and the eluent was immediately neutralized with 15 μL of Tris-HCl (pH 9.1) to prevent destruction of the phages.

The eluted phages were amplified using *E. coli* ER2738 to make sufficient copies for subsequent rounds of biopanning. The amplified phages were harvested by NaCl/polyethylene glycol precipitation. After each round of biopanning, the recovered phages were titered by plating aliquots of the infected *E. coli* ER2738 prior to amplification on Luria–Bertani (LB, BD Biosciences, San Jose, CA, USA) agar containing isopropyl β-D-1-thiogalactopyranoside (IPTG) and X-gal. The percent yield of bound phages was calculated as follows: output phage/input phage × 100.

2.5. Binding assay for specific peptide to NGAL

To evaluate whether the selected phage clones can specifically bind to NGAL, ELISAs were performed. Plates were coated with biotinylated NGAL for overnight incubation at 4 °C, blocked with blocking buffer,

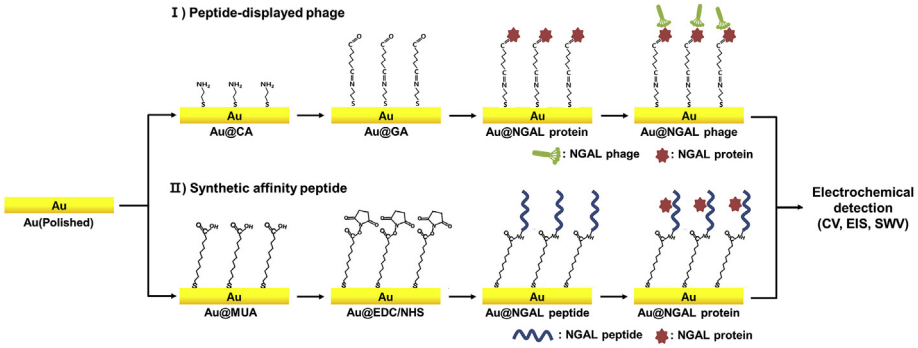

Scheme 1. A schematic illustration of the electrochemical sensor showing the principles of the phage and peptide sensor.

and washed six times with TBST solution. One hundred microliters of amplified phages (10^{11} pfu) were added to a plate, which was then incubated for 1 h at room temperature. After washing six times with the same buffer to remove unbound phages, HRP-conjugated anti-M13 monoclonal antibody (diluted 1:10,000 in blocking buffer) was added and the plate was then incubated for 1 h at room temperature. The antibody solution was removed, and the plate was washed again with TBST. Freshly prepared HRP substrates were added to the plate and the ELISA signal was measured at 405 nm using a microplate spectrophotometer (Multiskan FC, Thermo Scientific, Waltham, MA, USA).

2.6. Preparation of peptide-displayed phage sensor

A peptide-functionalized gold working electrode was prepared by the following steps. First, the gold electrode (1 × 2 cm) was immersed in piranha solution (H_2SO_4:H_2O_2 = 7:3, v/v) to remove dust and impurities on the surface of the gold electrode for around 10 min. Next, the electrode was rinsed with deionized (DI) water several times and sonicated in DI water for 1 min. The pre-treated electrode was dried by blowing N_2 gas for several seconds. After the polishing steps, the electrode was soaked in 50 mM cysteamine for overnight at darkness and immersed in 5% glutaldehyde for 1 h. After washing with DI water, pretreated electrode was incubated with 1 μg/mL of NGAL protein for 1 h at room temperature. Finally, NGAL pre-coated electrode was reacted with peptide-displayed phage particles, and the binding affinity was measured by EIS and SWV.

2.7. Preparation of the affinity peptide-functionalized gold electrode

The preparation of gold electrode was performed the same procedure before cysteamine and glutaldehyde treatment, as aforementioned above. After the polishing steps, the electrode was soaked 1 mL of MUA (1 mM) for 3 h at room temperature. After washing the electrode briefly, the solution (400 mM of EDC and 100 mM of NHS) was coated on the electrode for 30 min and then the electrode and voltammetric cell were assembled together. 75 μL of synthetic peptide (100 μg/mL) was dropped onto the gold electrode, which was then incubated 1 h at room temperature. The cell was washed with 1X phosphate-buffered saline (PBS, pH 7.4) and distilled water to remove unbound peptides. Next, 50 μL of NGAL proteins were loaded on the assembled cell, which was then incubated for 1 h at room temperature. The cell was then sequentially washed with 1X PBS and distilled water to remove unbound NGAL proteins.

2.8. Circular dichroism (CD) spectroscopy

The CD spectra of all of the synthetic peptide solutions with a concentration of 50 μM were recorded with a CD spectrometer (J-715, JASCO) using a UV cell with an optical path length of 0.1 cm at 25 °C. In the CD experiments, phosphate-buffered saline (PBS, pH 7.4) solution was used and the CD spectra were scanned 4 times, as has been previously reported (Hwang et al., 2017).

2.9. CV, EIS, and square-wave voltammetry (SWV) for the detection of NGAL

A conventional three-electrode cell including the aforementioned gold working electrode, a platinum counter electrode, and an Ag/AgCl reference electrode was used for the electrochemical measurements. CV, EIS, and SWV were performed using an electrochemical analyzer (CHI 750E, CH Instruments), connected to a computer data analysis system. These analyses were conducted in a PBS solution with 4 mM of ferro/ferricyanide. CV was recorded from −0.8 to +0.4 V vs. Ag/AgCl electrode at a sweep rate of 500 mV/s, while SWV was used to measure the electrochemical behavior after each preparation under the following conditions: amplitude 5 mV, potential range −0.8 V to +0.8 V, with scan increments of 4 mV, at a frequency of 10 Hz. EIS was carried out at a formal DC potential of 0.2 V using an alternating voltage of 10 mV in the frequency range from 100 kHz to 1 Hz. In the SWV experiments, the decrease in peak current was calculated based on the relative current change (ΔI %) by considering the peak current change obtained after peptide immobilization and NGAL protein interaction of SWV voltammograms recorded using the relationship (Meirinho et al., 2017)

$$\Delta I\ \% = (I_b - I_a)/I_b \times 100 \quad (1)$$

where ΔI is the relative current change (%) and I_b and I_a represent the current before and after sample incubation, respectively. In the EIS measurements, the relative R_{ct} signal changed according to the increased binding of NGAL to the synthetic peptides.Therefore, R_{ct} could be calculated by the following equation (Lim et al., 2017):

$$\Delta R_{ct} = (R_{ct,\ protein} - R_{ct,\ peptide})/R_{ct,\ peptide} \times 100 \quad (2)$$

where, $R_{ct,\ peptide}$ is the mean value of R_{ct} after immobilization of the peptides only (no addition of target protein), and $R_{ct,\ protein}$ the mean value of R_{ct} after addition of the target proteins.

2.10. SEM analysis

Field emission scanning electron microscope (FE-SEM) was performed with a Carl Zeiss Sigma HD instrument in Korea Research Institute Chemical Technology (KRICT) to examine the immobilization of affinity peptide on a gold surface. In detail, the images were observed by in-lens detector after Pt coating with a Cressington sputter coater for 120 sec to minimize denaturation on an accelerating voltage of 5 kV and working distances of 2.0 mm.

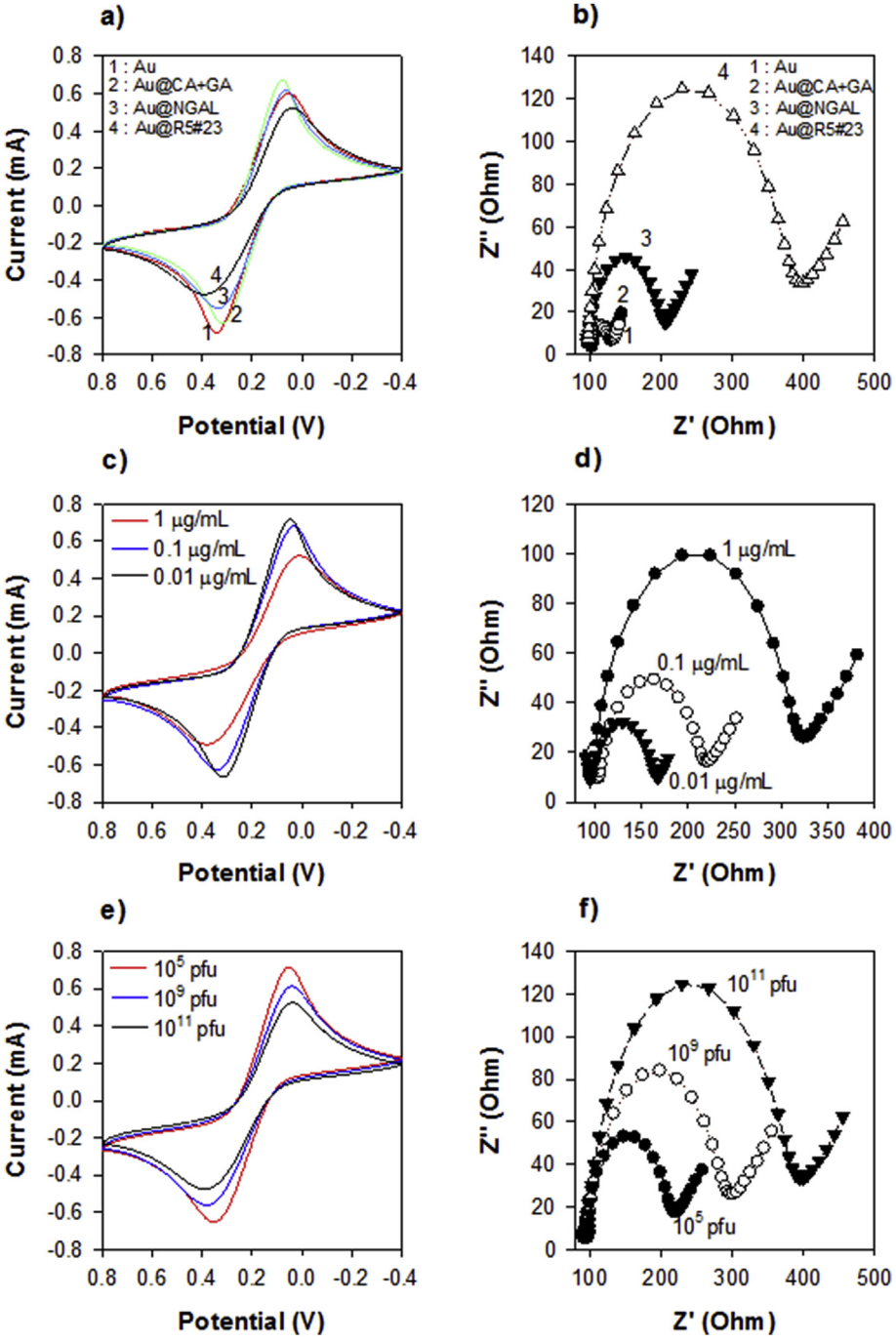

Fig. 1. Characterization and performance of the electrochemical phage sensor were monitored by performing CV (a, c, e) and EIS (b, d, f) after immobilization (1, bare gold (Au); 2, gold/cysteamine–glutaraldehyde (Au@CA + GA); 3, NGAL immobilization (Au@NGAL); and 4, NGAL 5#23 phage (Au@R5#23). (For interpretation of the references to colour in this figure legend, the reader is referred to the Web version of this article.)

3. Results and discussion

3.1. Identification of unique affinity peptides specific for NGAL using phage display

Briefly, biotinylated recombinant human NGAL was immobilized on a streptavidin-coated microwell plate and washed with TBST after blocking with 1% of BSA. Ph.D.-12 phage display random peptide library (1.5×10^{13} pfu) was reacted with the immobilized NGAL in the pre-coated well and bound phages were eluted. NGAL-specific peptides were identified after five rounds of biopanning, the enrichment after which is reported in Table S1. Samples of the eluted phages from each round of biopanning were analyzed by performing DNA sequencing. While performing biopanning, we selected two interesting phage clones, namely NGAL R5#9 with amino acid sequence GDGNSVLKP-GNW and NGAL 5#23 with amino acid sequence DRWVARDPASIF, and determined their relative binding affinities toward NGAL by performing ELISA, the results of which are shown in Fig. S1a: NGAL 5#23 showed the best affinity for NGAL compared with NGAL 5#9. Based on the sequence analysis results, uncharged hydrophobic amino acid residues such as Trp, Val, Ala, Pro, Ile, and Phe were rich in NGAL 5#23. These hydrophobic (like Trp) and negatively charged (like Arg) residues could be involved in π-π and/or cation-π interactions, suggesting that they may play an important role in binding to NGAL (Sawada et al., 2013).

In addition, sequence analysis detected two Asp residues at positions 1 and 7 and two Arg residues at positions 2 and 7. Therefore, we selected the NGAL 5#23 phage clone as a promising candidate for performing further experiments.

3.2. Characterization of the binding interaction of the peptide-displayed phage clones with NGAL

To investigate the effect of phage particle concentration on binding interactions, different concentrations (10^5–10^{11} pfu/mL) of the NGAL 5#23 phage clone were incubated with 7.6 μg/mL NGAL and changes in ELISA signal were examined. Fig. S1b shows the relative binding affinity of the NGAL 5#23 phage clone at different phage concentrations; it showed the highest binding affinity at a concentration of 10^{11} pfu/mL which sharply decreased at concentrations below this. This might have been a cause of the loss of avidity (Park et al., 2010). Thus, we confirmed that the NGAL 5#23 phage-displayed peptide could specifically bind to NGAL.

To assess the effects of NGAL concentration on binding interactions, approximately 10^{11} pfu/mL NGAL 5#23 phage clones were added to streptavidin-precoated wells containing different concentrations of NGAL (1–60.5 μg/mL), after which ELISA signals were measured (Fig. S1c). The binding affinity of the NGAL 5#23 clone increased with an increase in the concentration of NGAL and reached saturation at a concentration of 60.5 μg/mL. Interestingly, the NGAL 5#23 clone showed a strong binding affinity at an NGAL concentration of as low as 1 μg/mL. As expected, the ELISA signal with BSA as the control was quite low. Fig. S1d shows the relative binding affinity of the NGAL 5#23 clone toward NGAL in the presence or absence of serum. Interestingly, it could bind to NGAL at 1% serum concentration, but its binding affinity toward NGAL decreased slightly at serum concentrations of up to 2% and rapidly decreased at 10%. These observations indicate that the presence of serum had a limited effect on the binding interaction between the phage-displayed peptides and NGAL but affected the binding affinity of phage-displayed NGAL 5#23 peptides toward NGAL.

As a proof-of-principle, we constructed an electrochemical phage sensor for detecting NGAL. The surface layer of a gold electrode was modified as follows. (i) The gold electrode was immersed in a cysteamine solution (50 mM) and was incubated overnight in the dark. (ii) After washing the electrode with PBS buffer, 5% glutaraldehyde solution and 100 μL NGAL (5 μg/mL) were applied to the cysteamine-modified electrode and the electrode was incubated for 1 h (iii) After washing sequentially with PBS buffer and DI water to remove residual reagents, live phage particles (10^{11} pfu/mL NGAL 5#23 phage particles) were incubated with the functionalized gold electrode for 1 h, after which the electrode was washed again with the same buffer. Finally, the performance and binding affinity of the sensor were monitored by performing CV and EIS (Fig. S2). Fig. 1 shows the performance of the electrochemical phage sensor for detecting NGAL, as determined by performing CV (Fig. 1a, c, and 1e) and EIS (Fig. 1b, d, and 1f). The results indicate that the electrochemical phage sensor was successfully constructed using the surface-chemistry strategy (Fig. 1a and b) and that the sensor was active and specific for NGAL. We clearly observed a dynamic decrease in the current and a quantitative increase in the impedance when NGAL 5#23 phage particles were added onto the functionalized gold electrode layer.

Next, we examined the effects of NGAL concentration on the electrochemical phage sensor. Increasing the NGAL concentration (0.01, 0.1, and 1 μg/mL) decreased the current (Fig. 1c) and increased the impedance (Fig. 1d) due to the fact that the phage-displayed peptides could specifically bind to NGAL. Thus, our results indicate that the phage sensor was successfully developed using the multiple surface-chemistry strategy and that the sensor was specific for NGAL at a concentration of 1 μg/mL (Fig. 1c). To assess the effect of phage concentration on binding interactions, the functionalized gold electrode was treated with different phage concentrations (10^5, 10^9, and 10^{11} pfu/mL of NGAL 5#23 phage particles) and CV and EIS were performed to determine the changes in current and impedance, respectively (Fig. 1e and f). The EIS results show that the binding of the phage-displayed peptides to NGAL increased the impedance, suggesting that the interaction of the peptides displayed (five copies of the peptides per phage) with NGAL was specific.

These noteworthy results indicate that the phage-displayed peptides are robust and can be easily incorporated with other recognition reagents (probes) such as biomolecules and nanoparticles. The use of phage particles is fascinating because (i) the mass production of phages is cost-effective, (ii) affinity peptides identified by using the phage display technique are smaller than antibodies, and (iii) free peptides separated from phage particles can be easily synthesized to create peptide libraries for developing biosensors. Our results suggest that electrochemical phage sensors can be used as alternative biorecognition elements in various biosensing platforms.

3.3. Secondary structure analysis of synthetic peptides on binding interactions

To apply the affinity peptide in an electrochemical protein biosensor, a series of cysteine-incorporated free peptides specific for NGAL isolated from phage particles were chemically synthesized with high purity (> 95%), as reported in Table 1. In detail, the NGAL BP1 peptide has an amino acid sequence of DRWVARDPASIFGGGGSC, and we incorporated Cys at the C-terminus for a thiol self-assembled monolayer and a linker (-GGGGS-) for molecular flexibility on the gold surface. To study the effects of neutral amino acid composition on binding interactions, Asp at positions 1 and 6 of the NGAL BP1 were first replaced by neutral amino acids (like Lys) to create NGAL BP2 with an amino acid sequence of KRWVAKDPASIFGGGGSC. Second, the selected 12-mer unique peptide (DRWVARDPASIF) was repeated twice to create the NGAL BP3 peptide with an amino acid sequence of DRWVARDPASIF-DRWVARDPASIFGGGGSC. Third, the selected 12-mer unique peptide was reversed to create NGAL BP4. Finally, a non-fouling peptide (-EKEKEKE-) and two repeated flexible linkers (-GGGGS-) were incorporated in the sequence to create NGAL BP5.

CD spectroscopy was used to study the secondary structures of the synthetic peptides. The molar ellipticity values of the NGAL BP1 and BP3 peptides were mostly similar but not identical random coil structures (Fig. S3). The analysis of NGAL BP2, BP4, and BP5 showed that

Table 1
Amino acid sequences of the synthetic peptides used in this study.

Name	Amino acid sequence	Mass (MS found)	Notes
NGAL BP1	DRWVARDPASIFGGGGSC	1850	Selected after biopanning. Used as a scaffold for the rational design of the other peptides.
NGAL BP2	KRWVAKDPASIFGGGGSC	1835	Substitution of D and R in positions 1 and 6 to K. To analyze the effect of neutral amino acids on binding interaction.
NGAL BP3	DRWVARDPASIFDRWVARDPASIFGGGGSC	3166	Two repeats of NGAL BP1
NGAL BP4	FISAPDRAVWRDGGGGSC	1850	Reverse sequence of NGAL BP1
NGAL BP5	DRWVARDPASIFEKEKEKEGGGGSGGGGSC	2967	Incorporation of the non-fouling peptide EKEKEKE and two repeats of the flexible linker GGGGS.

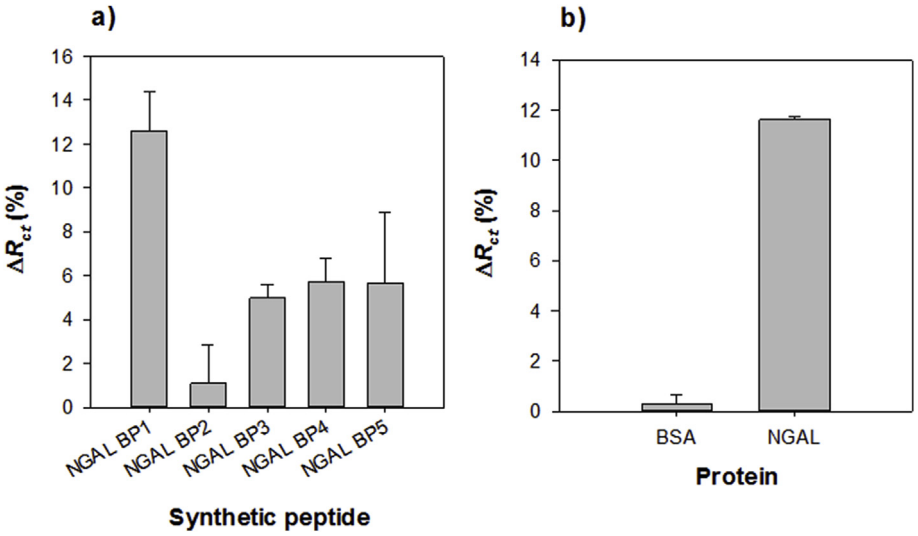

Fig. 2. (a) Selection of NGAL-specific synthetic peptides and (b) specificity testing performed using EIS measurements.

their ellipticity values were also similar but not identical. It is noteworthy that the NGAL BP1 peptide was able to form a random coil structure and it includes rich non-polar amino acids such as Trp, Ala, Ile, and Phe as well as Pro residues. From these observations, we suggest that non-polar residues with a random coil structure and the Pro hinge are necessary for specific binding to NGAL proteins.

3.4. Selection of the best synthetic peptides for NGAL

For determining the best synthetic peptides specific to NGAL proteins, the relative binding affinities of five synthetic peptide analogs (NGAL BP1–BP5) were compared via EIS measurements (Fig. 2a). Briefly, NGAL BP1–BP5 were rationally designed, chemically synthesized, and modified with a C-terminal cysteine and a linker (-GGGGS-) for molecular flexibility. After peptide treatment, SEM revealed the successful immobilization on gold surface layer, while the bare gold exhibited an original gold surface morphology (Fig. S4). For selection, 100 μg/mL each synthetic peptide was immobilized onto the gold sensor layer, washed three times with DI water, and incubated with NGAL proteins (7.5 μg/mL). The binding affinities of the series of synthetic peptides were determined by comparing the interaction of the NGAL protein with each peptide on a pre-immobilized gold surface layer and were observed as a change in impedance using EIS. Among the peptides, NGAL BP1 produced the greatest increase in impedance (highest affinity for NGAL), while NGAL BP2 had the lowest binding affinity for NGAL. However, the binding affinity of NGAL BP3 was comparable to BP4 and BP5, which was not expected since it was designed with two repeats of the selected peptide sequence and it was assumed that its binding affinity for NGAL would increase due to more of the binding motif. Interestingly, the binding affinity of NGAL BP2 was relatively low. From these observations, we learned that replacement by neutral amino acids (like Lys) could be dominant factors for the binding of NGAL. In fact, the relative binding affinity of the peptides followed the trend NGAL BP1 > NGAL BP5 > NGAL BP4 > NGAL BP3 > NGAL BP2.

These results indicate the successful immobilization of the affinity peptides and the binding of NGAL on the sensor layer, thereby providing for the sensitive recognition of NGAL. From these observations and more interestingly, NGAL BP1 was quite specific for NGAL and did not bind to BSA (the control) (Fig. 2b), we chose it as the most promising affinity peptide for the detection of NGAL.

3.5. Optimization of the sensor

After selecting the best peptide, SWV and EIS measurements were used to investigate the effects of NGAL BP1 concentration on binding interaction. The dynamic peak response of varying concentrations (from 1 to 100 μg/mL) on a gold electrode layer was measured before and after incubation with NGAL (7.5 μg/mL). The change in current was calculated based on the relative current change (ΔI %), considering the peak current values of the SWV voltammograms obtained after covalent peptide immobilization and protein incubation. The ΔI % value increased with increasing concentrations of NGAL BP1 up to 25 μg/mL and reached saturation at 100 μg/mL (Fig. 3a). For EIS, the value of ΔR_{ct} increased up to concentrations of 10 μg/mL and decreased in the range of 25–100 μg/mL (Fig. 3b). Therefore, an NGAL BP1 peptide concentration of 10 μg/mL was selected as the optimum concentration for subsequent experiments.

To further optimize the NGAL protein concentration with respect to binding interactions, 10 μg/mL of NGAL BP1 with NGAL protein concentrations ranging from 0.001 to 7.5 μg/mL was incubated on a gold surface layer. The immobilization of NGAL BP1 resulted in increases in ΔI % and ΔR_{ct} in SWV (Fig. 3c) and EIS (Fig. 3d), respectively, and from the observations, both ΔI % and ΔR_{ct} value increased in a concentration-dependent manner. The sensitivity of the sensor system was evaluated by taking into account the ΔI % and ΔR_{ct} values for different NGAL concentrations. As can be seen in Fig. 3e and f, respectively, the ΔI % and ΔR_{ct} values were highly correlated with increasing NGAL concentration (from 0.0001 μg/mL to 7.5 μg/mL, regression coefficient $R^2 = 0.8642$ for SWV). The limit of detection (LOD) calculated using the equation $LOD = 3 \times \sigma/S$, where σ is the standard deviation and S is the sensitivity, was found to be 3.93 ng/mL in the SWV experiment, while EIS had a LOD of 1.74 ng/mL. Importantly, strong linearity with good correlation (regression coefficient $R^2 = 0.9751$) between ΔR_{ct} and NGAL concentration was seen in ranging from 0.0001 μg/mL to 7.5 μg/mL for EIS (Fig. 3f). The sensor response and accuracy with SWV and EIS were shown in Table S2. The coefficient of variation (COV) in SWV measurement ranged from 7% to 16% with relative standard deviation (0.41–2.15), while COV in EIS varied from between 4% and 16% with relative standard deviation (0.14–1.91). These results demonstrated that our peptide-incorporated electrochemical sensor was highly accurate and reproducible. Although both SWV and EIS produced similar LOD values, EIS is preferable due to a larger linear dynamic range. As we previously found, EIS appears to be the optimal electrochemical method for the detection of procalcitonin (Lim et al., 2017) and troponin I (Wu et al., 2011), because it is straightforward and high

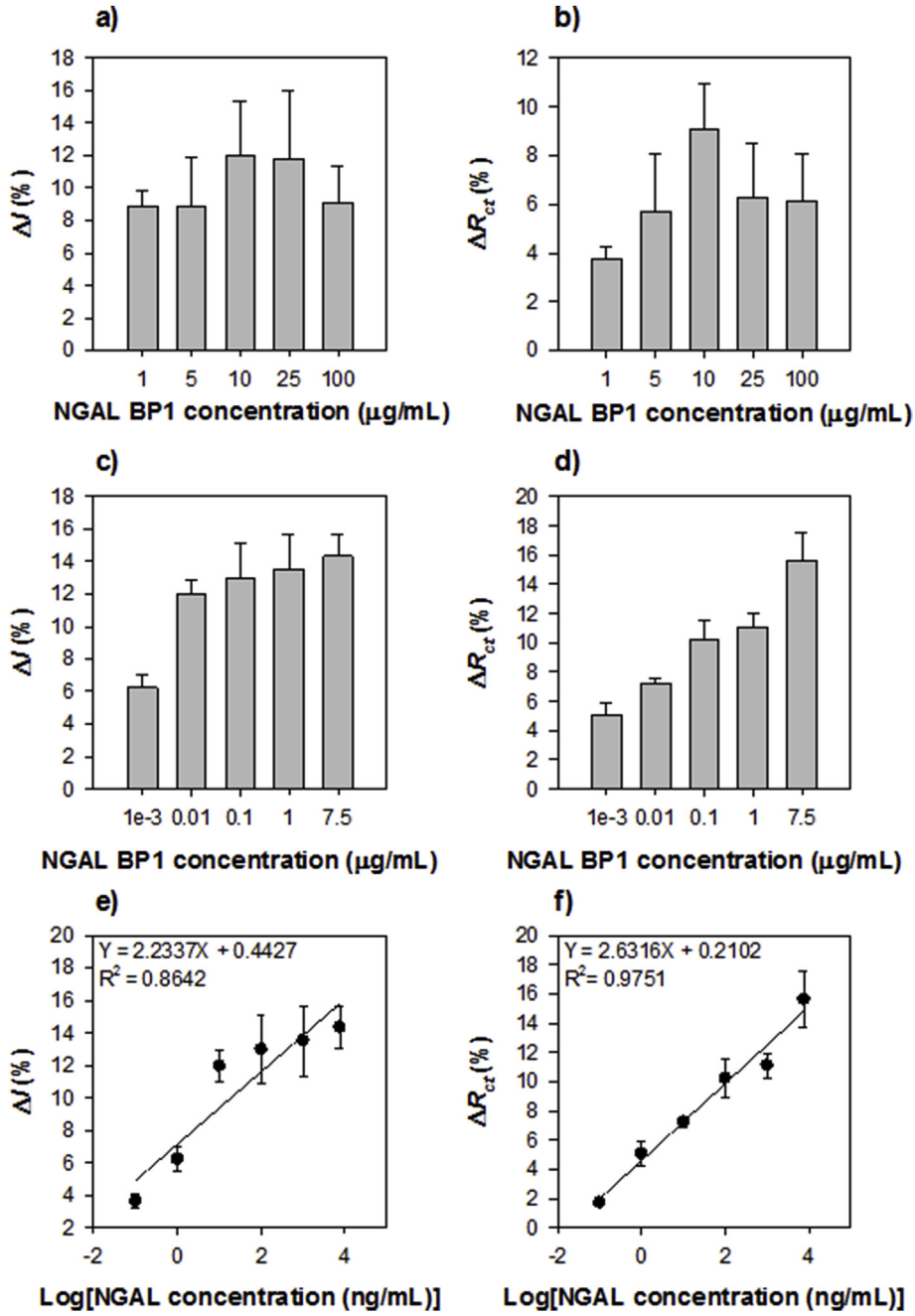

Fig. 3. SWV (a–c) and EIS (d–f) electrochemical measurements used to characterize the binding affinities of the NGAL BP1 peptide for the detection of NGAL. Optimization of the NGAL BP1 peptide concentration (a, d), the effect of NGAL protein concentration on binding interaction (b, e), and the electrochemical performance of NGAL BP1 for the detection of NGAL (c, f).

sensitivities with low LOD.

In order to see the stability of the developed sensor, NGAL BP1 (10 μg/mL)-immobilized electrodes were incubated with NGAL protein (7.5 μg/mL) at 4 °C for up to 5 h. The change in impedance was measured using EIS from 0 to 5 h. It was found to be stable for 5 h, with only a little loss in the initial state over whole time period (Fig. S5).

3.6. The validation of the sensor

An efficient and label-free biosensor system has been described as playing an important role in real clinical tests for early diagnosis. Therefore, the applicability of a bioanalytical technique when assaying in crude blood or plasma is necessary for the rapid and accurate diagnosis of target diseases. NGAL is a small protein (~25 kDa) in size that belongs to the lipocalin protein family and primarily produced in the renal tubules in response to structural kidney injury (Belcher et al., 2014; Pal et al., 2016; Eilenberg et al., 2017). A recent study has suggested that the level of NGAL can be used not only as a biomarker for early renal damage in type 1 diabetic nephropathy but also as an early predictor of AKI in the clinical setting (Eilenberg et al., 2017). Therefore, we hypothesized that NGAL detection could be used for the early diagnosis of diabetic nephropathy.

Both ELISA and EIS were performed to compare the performance of NGAL detection using crude plasma from a normal group ($n = 6$), prediabetic patients ($n = 6$), and diabetic patients ($n = 6$), and changes in ELISA signal (Fig. 4a) and impedance (ΔR_{ct} value, Fig. 4b) for EIS after the addition of plasma samples was measured. As expected, the level of NGAL concentration could be easily detected in the normal, pre-

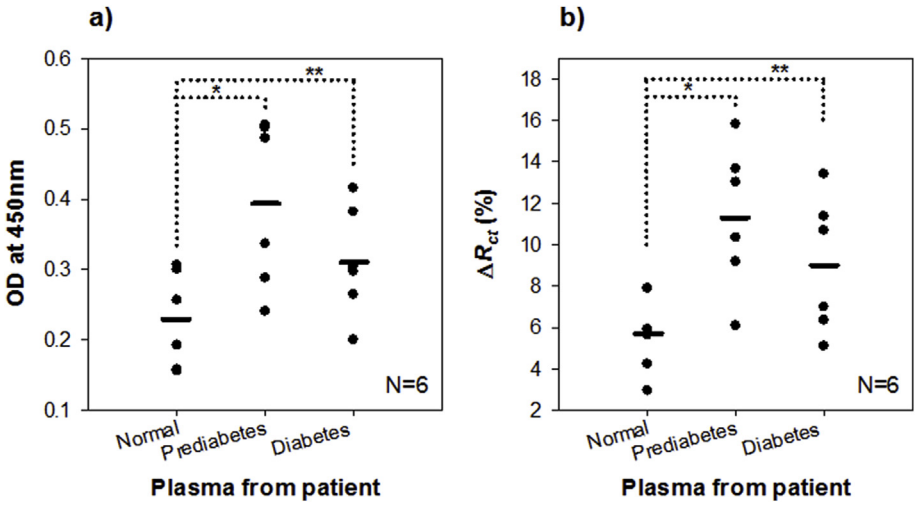

Fig. 4. Analytical performance for the detection of NGAL: a commercially available ELISA NGAL detection kit (a) compared to our sensor system (b). Statistical significance between groups was determined by ANOVA test, where p value is * $p < 0.02$ or ** $p < 0.256$ in Fig. 4a, * $p < 0.017$ or ** $p < 0.246$ in Fig. 4b, respectively. Mean values of each group are indicated with bold lines.

diabetic, and diabetic groups with a commercially available ELISA kit. In both cases, NGAL levels were significantly elevated in pre-diabetic, and diabetic groups compared to normal group. More interestingly, the ΔR_{ct} values measured in EIS for the plasma samples of each group were significantly different, indicating its usefulness for monitoring progression of diabetes. In fact, the ΔR_{ct} values for each group of plasma samples incubated on a gold electrode surface layer showed little variation in impedance change (Fig. 4b) compared to the ELISA results. Based on the slope of the calibration curve in our sensor with relationship ΔR_{ct} and NGAL concentration, it was found that the level of NGAL protein in normal, prediabetes and diabetic groups was 21.09, 42.34, and 33.37 ng/mL, respectively. As shown in Table S3, most of the coefficient of variation (COV) was below 15%, however, COV in diabetic group was little high. These may be due to the heterogeneous characteristics derived from patient-to-patient variation with different gender, body weight and age. These results showed that peptide-incorporated sensor for NGAL detection was reproducible and accurate. The comparison of sensor performance between commercially available ELISA kit and our sensor was summarized in Table S4.

4. Conclusion

In this work, we used a phage display technique to successfully identify novel peptides specific for NGAL. The peptide specific for NGAL binding (NGAL 5#23) had an amino acid sequence of DRWARDPASIF, and ELISA, CV, SWV, and EIS were performed to evaluate its binding affinity toward NGAL. NGAL 5#23 phage particles were active in the presence of high serum concentrations. Moreover, we successfully generated an electrochemical phage sensor by using a general surface-chemistry approach on a gold electrode. The performance of the electrochemical phage sensor was evaluated by performing CV and EIS, the respective results of which showed clear quantitative decrease in current and increase in impedance with an increase in NGAL concentration. From the results of ELISA, SWV, and EIS analyses of NGAL BP1–BP5, NGAL BP1 was selected as the most promising recognition receptor and its binding affinity were observed via SWV and EIS analyses. Our results show that the peptide sensor system could detect NGAL with high sensitivity and selectivity with a detection performance comparable to a commercially available ELISA NGAL detection kit. The applicability of the peptide sensor for the detection of NGAL in plasma from patient samples was confirmed by the ΔR_{ct} values of the sensor layer incorporating NGAL BP1 peptides showing a statistically significant difference.

Compared to more complex antibody-based immunoassay, short peptides have several advantages that can be applied for biosensor development. i) peptides can be rationally designed and easily synthesized, ii) peptides can be more amenable than antibodies to engineering at the molecular level, iii) peptides are more stable and resistant under harsh conditions. Since phage display and electrochemical detection regime are well-known and widely used, this approach is straightforward for biosensor development. These suggest the potential use of our biosensing platform for monitoring NGAL as a miniaturized electrochemical biosensor for the early monitoring of diabetes nephropathy.

Declaration of interests

The authors declare that they have no known competing financial interests or personal relationships that could have appeared to influence the work reported in this paper.

CRediT authorship contribution statement

Chae Hwan Cho: Formal analysis, Writing - original draft. **Ji Hong Kim:** Formal analysis, Writing - original draft. **Dae-Kyu Song:** Formal analysis, Writing - original draft. **Tae Jung Park:** Formal analysis, Writing - original draft. **Jong Pil Park:** Formal analysis, Writing - original draft.

Acknowledgements

This study was supported by the National Research Foundation of Korea grant funded by the Korea government (MSIP) (NRF-2017R1A2A2A05001037).

Appendix A. Supplementary data

Supplementary data to this article can be found online at https://doi.org/10.1016/j.bios.2019.111482.

References

Barrera-Chimal, J., Bobadilla, N.A., 2012. Biomarkers 17 (5), 385–393.
Belcher, J.M., Sanyal, A.J., Peixoto, A.J., Perazella, M.A., Lim, J., Thiessen-Philbrook, H., Ansari, N., Coca, S.G., Garcia-Tsao, G., Parikh, C.R., 2014. Hepatology 60 (2), 622–632.
Bjornstad, P., Snell-Bergeon, J.K., Lovshin, J.A., Singh, S.K., Lovblom, L.E., Tse, J.M., Orszag, A., Lytvyn, Y., Brent, M.H., Paul, N., Weisman, A., Keenan, H.A., Cham, L., Bril, V., Perkins, B.A., Cherney, D., 2018. Diabetes 67 (Suppl. 1), 520.
Bonventre, J.V., 2007. Contrib. Nephrol. 156, 213–219.
Choi, J., Jeun, M., Yuk, S.-S., Park, S., Choi, J., Lee, D., Shin, H., Kim, H., Cho, I.-J., Kim, S.K., Lee, S., Song, C.S., Lee, K.H., 2019. ACS Nano 13 (1), 812–820.
Coca, S.G., Yalavarthy, R., Concato, J., Parikh, C.R., 2008. Kidney Int. 73 (9), 1008–1016.
Crivianu-Gaita, V., Thompson, M., 2016. Biosens. Bioelectron. 85, 32–45.
Eilenberg, W., Stojkovic, S., Piechota-Polanczyk, A., Kaider, A., Kozakowski, N.,

Weninger, W.J., Nanobachvili, J., Wojta, J., Huk, I., Demyanets, S., Neumayer, C., 2017. Cardiovasc. Diabetol. 16 (1), 98.
Endre, Z.H., Pickering, J.W., 2014. Nat. Rev. Nephrol. 10 (12), 683–685.
Han, W.K., Waikar, S.S., Johnson, A., Betensky, R.A., Dent, C.L., Devarajan, P., Bonventre, J.V., 2008. Kidney Int. 73 (7), 863–869.
Hassanzadeh, M., Ghaemy, M., 2017. New J. Chem. 41 (6), 2277–2286.
Heo, N.S., Oh, S.Y., Ryu, M.Y., Baek, S.H., Park, T.J., Choi, C., Huh, Y.S., Park, J.P., 2019. Biotechnol. Bioproc. E. 24 (2), 318–325.
Hwang, H.J., Ryu, M.Y., Park, C.Y., Ahn, J., Park, H.G., Choi, C., Ha, S.-D., Park, T.J., Park, J.P., 2017. Biosens. Bioelectron. 87, 164–170.
Hwang, H.J., Ryu, M.Y., Park, J.P., 2015. RSC Adv. 5 (68), 55300–55302.
Ki, M.K., Kang, K.J., Shim, H., 2010. Biotechnol. Bioproc. E. 15 (1), 152–156.
Lee, D., Hwang, J., Seo, Y., Gilad, A.A., Choi, J., 2018. Biotechnol. Bioproc. E. 23 (2), 123–133.
Li, H., Mu, Y., Yan, J., Cui, D., Ou, W., Wan, Y., Liu, S., 2015. Anal. Chem. 87 (3), 2007–2015.
Lim, J.M., Ryu, M.Y., Kim, J.H., Cho, C.H., Park, T.J., Park, J.P., 2017. RSC Adv. 7 (58), 36562–36565.
McCullough, P.A., Shaw, A.D., Haase, M., Bouchard, J., Waikar, S.S., Siew, E.D., Murray, P.T., Mehta, R.L., Ronco, C., 2013. Contrib. Nephrol. 182, 13–29.
Meirinho, S.G., Dias, L.G., Peres, A.M., Rodrigues, L.R., 2017. Anal. Chim. Acta 987, 25–37.
Mousavi, M.Z., Chen, H.-Y., Lee, K.-L., Lin, H., Chen, H.-H., Lin, Y.-F., Wong, C.-S., Li, H.F., Wei, P.-K., Cheng, J.-Y., 2015. Analyst 140 (12), 4097–4104.
Pal, S., Lohar, S., Mukherjee, M., Chattopadhyay, P., Dhara, K., 2016. Chem. Commun. (J. Chem. Soc. Sect. D) 52 (94), 13706–13709.
Park, C.R., Park, S.J., Lee, W.G., Hwang, B.H., 2018. Biotechnol. Bioproc. E. 23 (4), 355–370.
Park, J.P., Cropek, D.M., Banta, S., 2010. Biotechnol. Bioeng. 105 (4), 678–686.
Park, J.P., Park, C.Y., Park, A.Y., Ryu, M.Y., 2015. RSC Adv. 5 (110), 90531–90533.
Parmar, A.K., Valand, N.N., Solanki, K.B., Menon, S.K., 2016. Analyst 141 (4), 1488–1498.
Ribitsch, W., Schilcher, G., Quehenberger, F., Pilz, S., Portugaller, R.H., Truschnig-Wilders, M., Zweiker, R., Brodmann, M., Stiegler, P., Rosenkranz, A.R., Pickering, J.W., Horina, J.H., 2017. Sci. Rep. 7, 41300.
Sawada, T., Okeya, Y., Hashizume, M., Serizawa, T., 2013. Chem. Commun. (J. Chem. Soc. Sect. D) 49 (44), 5088–5090.
Sheanon, N.M., Mottl, A.K., Dagostino, R., Suerken, C., Afkarian, M., Dabelea, D., Imperatore, G., Marcovina, S.M., Pettitt, D.J., Saydah, S., Dolan, L.M., 2018. Diabetes 67 (Suppl. 1), 525.
Sidhu, S.S., Feld, B.K., Weiss, G.A., 2007. Methods Mol. Biol. 352, 205–219.
So Young, K.M.D., Tae-Dong, J., Woochang, L., Sail, C., Sung, S., Soon Bae, K., Won-Ki, M., 2018. Ann. Lab. Med. 38 (6), 524–529.
Soni, S.S., Ronco, C., Katz, N., Cruz, D.N., 2009. Blood Purif. 28 (3), 165–174.
Tai, T.-Y., Sinha, A., Sarangadharan, I., Pulikkathodi, A.K., Wang, S.-L., Lee, G.-Y., Chyi, J.-I., Shiesh, S.-C., Lee, G.-B., Wang, Y.-L., 2019. Anal. Chem. 91 (9), 5953–5960.
Teengam, P., Siangproh, W., Tuantranont, A., Henry, C.S., Vilaivan, T., Chailapakul, O., 2017. Anal. Chim. Acta 952, 32–40.
Waikar, S.S., Bonventre, J.V., 2007. Curr. Opin. Nephrol. Hypertens. 16 (6), 557–564.
Wu, J., Park, J.P., Dooley, K., Cropek, D.M., West, A.C., Banta, S., 2011. PLoS One 6 (10), e24948.
Yang, J.M., Kim, K.R., Kim, C.S., 2018. Biotechnol. Bioproc. E. 23 (4), 371–382.
Yoon, J.-Y., Kim, D.-H., Kim, S., Kim, D., Jo, G., Shin, M.-S., Yoo, J., Kang, H.K., Kim, M.S., Kim, Y.-J., Lee, N.-T., Hong, H.J., Kim, Y.-W., 2017. Biotechnol. Bioproc. E. 22 (2), 114–119.
Yukird, J., Wongtangprasert, T., Rangkupan, R., Chailapakul, O., Pisitkun, T., Rodthongkum, N., 2017. Biosens. Bioelectron. 87, 249–255.